Heliyon 9 (2023) e18698

Contents lists available at ScienceDirect

Heliyon

journal homepage: www.cell.com/heliyon

Lnc-PLA2G4A-4 facilitates the progression of hepatocellular carcinoma by inducing versican expression via sponging miR-23b-3p

Jiahui Xiong [a,b,d,1], Yongping Lai [b,e,1], Niangmei Cheng [b,e,1], Jizhe Liu [c,1], Fei Wang [b,e], Xiaoyuan Zheng [b,e], Yingchao Wang [b,e], Qiuyu Zhuang [b,e], Yantin Lin [a,b,d], Jingfeng Liu [f], Yixuan Yang [g], Bixing Zhao [b,e,*], Xiaoyu Yang [a,b,d,**]

[a] *Fuzhou Hospital of Traditional Chinese Medicine Affiliated to Fujian University of Traditional Chinese Medicine, Fuzhou 350001, PR China*
[b] *The United Innovation of Mengchao Hepatobiliary Technology Key Laboratory of Fujian Province, Mengchao Hepatobiliary Hospital of Fujian Medical University, Fuzhou 350025, PR China*
[c] *College of Life Science, Fujian Agriculture and Forestry University, Fuzhou, Fujian, 350002, PR China*
[d] *The School of Basic Medical Sciences, Fujian Medical University, Fuzhou 350122, PR China*
[e] *Fujian Provincial Clinical Research Center for Hepatobiliary and Pancreatic Tumors, Fuzhou 350025, PR China*
[f] *Department of Hepatopancreatobiliary Surgery, Fujian Medical University Cancer Hospital, Fujian Cancer Hospital, Fuzhou, Fujian, PR China*
[g] *Fuzhou Gezhi High School of Fujian, Fuzhou, PR China*

ARTICLE INFO

Keywords:
Hepatocellular carcinoma
Lnc-PLA2G4A-4
miR-23b-3p
Versican
Metastasis

ABSTRACT

Aberrant expression of long non-coding RNAs (lncRNAs) is associated with progression of multiple human cancers including hepatocellular carcinoma (HCC). However, the role of lncRNAs in HCC is not been fully understood. Our study aimed to investigate the biological function and potential molecular mechanism of Lnc-PAL2G4A-4 in HCC. In the current study, we show that Lnc-PLA2G4A-4 was significantly up-regulated in HCC tissues and high Lnc-PLA2G4A-4 expression was remarkably associated with tumor size, microvascular invasion and poor prognosis of HCC patients. Functionally, Lnc-PLA2G4A-4 positively regulated cell proliferation, invasion and migration in vitro, and facilitated lung metastasis of HCC in vivo. Mechanistically, Lnc-PLA2G4A-4 functioned as a competing endogenous RNA (ceRNA) to bind to miR-23b-3p and subsequently facilitate miR-23b-3p's target gene versican (VCAN) expression in HCC cells. Over-expression of miR-23b-3p could reverse Lnc-PLA2G4A-4 induced cell phenotypes in HCC and suppress versican expression of by rescue analysis. Collectively, Lnc-PLA2G4A-4 promotes HCC progression by targeting the miR-23b-3p/versican axis, which may be a potential biomarker and therapeutic target for HCC.

* Corresponding author. Mengchao Hepatobiliary Hospital of Fujian Medical University, 312 Xihong Road, Fuzhou 350025, PR China.
** Corresponding author. Fuzhou Hospital of Traditional Chinese Medicine Affiliated to Fujian University of Traditional Chinese Medicine, 102 Gudong Road, Fuzhou 350001, PR China.
E-mail addresses: bixingzhao@gmail.com (B. Zhao), yangxiaoyu683@163.com (X. Yang).
[1] The contributions of these authors are equal.

https://doi.org/10.1016/j.heliyon.2023.e18698
Received 25 April 2023; Received in revised form 20 July 2023; Accepted 25 July 2023
Available online 26 July 2023

1. Introduction

Hepatocellular carcinoma (HCC) is one of the most common, aggressive malignancies, and the third leading cause of cancer death worldwide [1]. Although significant progress has been made in the treatment of HCC in recent years, the 5-year survival rate is still unsatisfactory due to the high incidence of metastasis and recurrence [2]. Therefore, identifying novel therapeutic targets to inhibit HCC metastasis and exploring the underlying mechanism of HCC metastasis are essential to reduce recurrence and improve the overall prognosis of HCC patients after surgery.

Long non-coding RNAs (lncRNAs) are defined as transcribed RNA sequences with a transcript greater than 200 nucleotides in length and lacking protein coding potential [3]. To date, there are increasing evidences indicating that lncRNAs function in many biological processes, including epigenetic, transcriptional, and posttranscriptional regulation [4–6]. More and more lncRNAs are found to affect cell proliferation, apoptosis and metastasis and regulate the tumour micro-environment in HCC, thereby affect tumorigenesis and progression [7]. It has been reported that LncRNA SNHG14 promoted HCC progression by sponging miR-4673 to regulate SOCS1 expression [8]. Another study shown that Lnc-APUE promotes G1/S phase transition and tumor growth by regulating miR-20b/E2F1 Axis [9]. Although a lot of lncRNAs have been reported to participate in the progression of HCC, the roles of most lncRNAs in HCC are still unclear.

Versican (VCAN) is a major component of the extracellular matrix, which is involved in cell adhesion, proliferation, migration and angiogenesis [10]. The expression of versican is upregulated in a variety of malignancies, including liver cancers [11], lung cancers [12], breast cancers [13], gastric cancers [14], colon cancers [15], ovarian cancers [16] and bladder cancers [17], and play important roles in all aspects of malignant transformation and progression of tumors [18], including participation in the regulation of tumor cell proliferation, invasion and metastasis, angiogenesis and apoptosis. Moreover, a lot of studies showed that versican is regulated by miRNAs, such as miR-543 [19], miR-135a-5p [20], and miR-143 [21]. And a recently study indicated that lnc-VCAN-AS1 may regulate the expression of versican via targeting miRNA [22]. Whether lncRNA affects tumor progression via regulating the expression and activity of versican remains to be explored.

To identify lncRNAs involved in the tumorigenesis and progression of HCC, we use transcriptome analysis and RT-qPCR to compare the expression of Lnc-PLA2G4A-4 HCC tissue and adjacent non-tumor tissue. Then, several functional assays are performed to investigate the effect of Lnc-PLA2G4A-4 in HCC. We firstly reported the upregulation of Lnc-PLA2G4A-4 in HCC and the stimulative roles of Lnc-PLA2G4A-4 in HCC proliferation and metastasis. Moreover, we analyzed the mechanism of Lnc-PLA2G4A-4 in HCC. Our findings elucidated that the Lnc-PLA2G4A-4/miR-23b-3p/versican axis is a novel regulatory mechanism implicated in HCC occurrence and progression, which provides a new prognostic predictor and a therapeutic target for HCC.

2. Materials and methods

2.1. Clinical specimens

Totally, 105 patients with HCC were enrolled from November 2013 to July 2016 at Mengchao Hepatobiliary Hospital of Fujian Medical University. All the patients underwent curative resection at Mengchao Hepatobiliary Hospital of Fujian Medical University. Clinical and pathological diagnosis of HCC patients were made following the diagnostic criteria of the American Association for the Study of Liver Diseases. All enrolled patients provided written informed consent and this study was approved by the ethics committee of Mengchao Hepatobiliary Hospital of Fujian Medical University (2020-027-01).

2.2. TCGA data of HCC

All available TCGA data on HCC were obtained from the TCGA data portal (TCGA group, https://tcga-data.nci.nih.gov/tcga/). In September 2021, there were RNAseq data on 424 HCC samples, including 324 single tumor samples, 50 pairs of HCC and adjacent non-tumor liver tissues, and clinical data including survival time and survival status records of 370 patients (excluding 1 case without survival time and 3 cases of recurrence). The gene expression data were normalized using the RNA normalization method described in the TCGA NCI Wiki. The expression value of the Lnc-PLA2G4A-4 gene was collected for each case and was divided into the high-expression and the low-expression groups using the cut-off point. Kaplan-Meier survival analysis was used to determine the survival differences between the high-expression and low-expression subgroups, with *P*-values calculated using the log-rank test.

2.3. Cell culture

Human HCC cell line SNU398, SNU449, SK-Hep-1, Hep3B, HepG2/C3A, as well as Human Embryonic Kidney 293T (HEK-293T) cell line were purchased from the American Type Culture Collection (ATCC, USA). Human HCC cell lines SMMC-7721, Huh7, and normal human hepatocyte cell line LO2 were purchased from the Chinese Cell Bank of the Chinese Academy of Sciences (Shanghai, China). Hep3B cell line was cultured in Eagle's Minimum Essential Medium (MEM; HyClone, USA). SNU398, SNU449 cell line was cultured in RPMI-1640 (Gibco, USA). SMMC-7721, Huh7, SK-Hep-1, HepG2/C3A, LO2, and HEK-293T cell lines were cultured in Dulbecco's Modified Eagle Medium (DMEM; Gibco, USA). During the process of cell culture, we sterilized the experimental materials, and the experiments were performed according to strict aseptic operation; 1% penicillin and streptomycin (Gibco, USA) were added to the growth medium when necessary in an effort to prevent bacterial contamination in the medium. All of the cultured mediums contained 10% (v/v) fetal bovine serum (FBS; Gibco, USA). Cells were cultured in an atmosphere of 95% humidified air and 5% CO_2 at

37 °C.

2.4. RT-qPCR

Total RNAs isolated from fresh-frozen tissues and cultured cells were extracted using TransZol Up Plus RNA kit (Beijing TransGen Biotech Ltd., China) and quantified. Afterwards, 1 μg of total RNA was revise-transcribed into cDNA using the Transcriptor First Strand cDNA Synthesis Kit (Roche Ltd., Basel, Switzerland). The miRNA was revise-transcribed into cDNA using miRcute Plus miRNA First-Strand cDNA Kit (Beijing TransGen Biotech Ltd., China). Then, RT-qPCR was carried out under the following conditions: initial denaturation at 95 °C for 5 min, 40 cycles of 95 °C for 10 s, 60 °C for 30 s and 72 °C for 30 s. The miRNA expression was detected using miRcute Plus miRNA qPCR Kit (SYBR Green) (Beijing TransGen Biotech Ltd., China). The primer sequences of target genes are shown in Supplementary Table S1. The sequences of oligonucleotides in miRNA mimics, miRNA inhibitor are shown in Supplementary Table S2. The relative gene expression was normalized to the geometric mean of the housekeeping gene 18S rRNA and U6, and then calculated according to the Livak method (ΔΔCt) (Livak and Schmittgen, 2001).

2.5. Plasmids and transfection

Stable Lnc-PLA2G4A-4 over-expression in the SNU398, SK-Hep-1 and C3A cell lines was achieved by transduction with lentivirus encoding Lnc-PLA2G4A-4. pCDH-CMV-Lnc-PLA2G4A-4-EF1-copGFP-T2A-Puro was designed and synthesized by Sangon Biotech (Shanghai, China). SMMC-7721 cell line was transfected with shRNA against Lnc-PLA2G4A-4 (pLKO.1-GFP-puro-sh-Lnc- PLA2G4A-4, target sequence: 5'-GCTTTATATCCAGGCAAATTG-3') according to the manufacturer's instructions. The empty vectors were used as negative control. Afterwards, HEK-293T cells were co-transfected with lentivirus packaging plasmid (Invitrogen, Waltham, MA, USA) and corresponding plasmids respectively, using the Lipofectamine 3000 (Invitrogen, Waltham, MA, USA) according to the manufacturer's protocol. Opti-MEM (Gibco, USA) as harvest media from cells was centrifugated at 4,000g for 15 min at 4 °C and was filtered through a 0.22 μm filter to remove the cells. Virus was concentrated by ultracentrifugation. The supernatant was centrifuge at 76,618g for 90min at 4 °C in a Beckman SW32 rotor. After that, poured off the supernatant and drained the remaining liquid by resting the inverted tubes on paper towels. Finally, re-suspended the viral pellets in 150 μl of DMEM (Gibco, USA) and stored at −80 °C. When target cells approximately 60–80% confluent, add 50 μl virus and 1 μl Polybrene (Beijing Solarbio Science & Technology Co., Ltd, China) to each target cells well. Subsequently, the infection efficiency was observed by fluorescence microscopy. The transfected cells were further selected by medium containing 2 μg/ml puromycin (Sigma-Aldrich, St Louis, MO, USA) for 2–3 weeks. The over-expression or knockdown efficiency of all transfections was validated by RT-qPCR.

2.6. Cell counting Kit-8 (CCK-8) assay

HCC cells suspensions were added to a 96-well plate at a density of 1000–2000 cells in 100 μl of complete medium and cultured overnight. A total of 10 μl CCK-8 solution (TransGen Biotech Ltd., Beijing, China) was added to each well at different time points (0h, 24h, 48h, 72h, 96h). The absorbance at 450 nm was measured using a microplate reader (Molecular Devices, USA) after 2 h incubation.

2.7. Colony formation assay

SMMC-7721 and SK-Hep-1 cell lines were seeded in a six-well plate (2000 cells/well) and cultured with complete medium for 7–14 days. Cell colonies were fixed with 4% paraformaldehyde (Wuhan Servicebio Biotech Ltd., China) for 30 min and stained with crystal violet (Beyotime Biotechnology Ltd., Shanghai, China). Photographs were captured, and the colonies were quantified using Image J software.

2.8. In vitro migration and invasion assays

Cell migration and invasion assays were carried out on 24-well plates with transwell inserts (8-μm pore size; Millipore, Billerica, MA, USA). Matrigel-coated inserts were used in the invasion assay. In each assay, 2×10^5 HCC cells were seeded in 200 μl serum-free DMEM/1640 in the upper chamber of the wells, and 600 μl DMEM/1640 with 10% FBS was placed in the lower chamber. The cells were incubated for 18–36 h, and the migrating or invading cells on the lower membrane surface were fixed in 4% paraformaldehyde (Wuhan Servicebio Biotech Ltd., China) for 20 min and stained with crystal violet (Beyotime Biotechnology Ltd., Shanghai, China) for 40min. The migrating or invading cells were counted in five randomly selected fields under a microscope. Images were acquired at 200 × magnification.

Wound healing assay were carried out to evaluate cell migration. When cells grew in full monolayer on cover slips in Ibidi Culture-Inserts (Ibidi, Germany), gently unplug the culture-Inserts and washed with PBS. Then use DMEM/RPMI-1640 with 2% FBS to relapse the medium immediately. Phase contrast images were captured and marked 0 h. The width of wounds was measured in three-independent wound sites per group. Constantly observed the wounds until one of them healed, the cells were taken contrast images again. Relative migration of cells was calculated with the healing distance.

2.9. Western blot

Total proteins were extracted from tissue samples or HCC cells and dissolved in radio immunoprecipitation assay (RIPA) lysis buffer (Beijing Solarbio Science & Technology Co., Ltd., China) with phosphatase Inhibitor Cocktail (cat. no. 11697498 001; Roche Diagnostics, Germany) and phenylmethanesulfonyl fluoride (Shanghai Macklin Biochemical Ltd., China). All proteins were quantified using a bicinchoninic acid protein assay kit (Beijing Solarbio Science & Technology Co., Ltd., China) according to the manufacturer's instructions. Equal amounts (40 μg) of protein were fractionated on 8–10% sodium dodecyl sulphatepolyacrylamide gels electrophoresis (SDS-PAGE), and transferred to nitrocellulose (NC) membranes (Pall Corporation, Mexico) with electroblotting. After blocking with 5% nonfat milk for 1 h at room temperature, the membranes were incubated with primary antibodies against E-cadherin (CST, #3159, 1:1000), N-cadherin (CST, #13116, 1:1000), Vimentin (CST, #5741p, 1:1000), Snail (CST, #3879s, 1:1000), Slug (Biorbyt, Orb74769, 1:1000), ZEB2 (Biorbyt, RG219, 1:1000), Versican (Abcam, ab177480, 1:1000), AKT (CST, #4691p, 1:1000), Cyclin D1 (CST, #2978s, 1:1000), EGFR (CST, #4267s, 1:1000), P21 (CST, #2947s, 1:1000), p-AKT (phosphorylation site: Thr308, CST, #13038s, 1:1000), p-EGFR (phosphorylation site: Tyr1173, CST, #4407, 1:1000) and β-actin-HRP (Abcam, ab49900, 1:20 000) overnight at 4 °C. Then, the membranes were washed three times with 1 × TBS-T and incubated with horseradish peroxidase (HRP)-conjugated secondary antibodies at a 1:3000 dilution for 1h at room temperature. The blot signals were visualized using an enhanced chemiluminescence (ECL) reagent (Thermo, USA) and detected with ChemiDoc Imaging System (Bio Rad, USA). β-actin-HRP (1:20 000, Abcam, #ab49900) was used as a loading control.

2.10. Tumor xenograft model

SMMC-7721 cells stably transfected with sh-Lnc-PLA2G4A-4 or sh-NC were harvested at the exponential growth stage and injected into the lateral tail veins of 5-week-old B-NDG mice (cat. no. 110586; Beijing Biocytogen Co., Ltd.). B-NDG mice were randomly divided into two groups of 5 animals each. Each immune-deficient mouse injected 200 μl cell suspension containing 2 × 10^6 cells. After 6 weeks, mice were sacrificed, and fluorescent images were taken by ChemiDoc Imaging System (Bio Rad, USA). Then, the resected lung tissues were fixed in 4% paraformaldehyde fix solution (Wuhan Servicebio Biotech Ltd., China). The fixed samples were embedded in paraffin and stained with hematoxylin and eosin (H&E staining). The relative fluorescence intensity of lung metastatic nodules was analyzed. All animal experiments were performed in accordance with guidelines of the Laboratory Animal Center of Fujian Medical University.

2.11. Luciferase reporter assay

The interaction between Lnc-PLA2G4A-4 and miR-23b-3p was measured using pGL3-Basic system. The interaction between versican and miR-23b-3p was measured using pmiRGLO system. Full length of Lnc-PLA2G4A-4 (termed Lnc-PLA2G4A-4 -WT) and mutated Lnc-PLA2G4A-4 (mutated in each miR-23b-3p target site of the Lnc-PLA2G4A-4 sequence, termed Lnc-PLA2G4A-4-Mut) were inserted into pGL3-Basic vector respectively. The 3'UTR region of versican were inserted into pmiRGLO vector. Luciferase reporter assays were performed according to the manufacturer's instruction. Briefly, HEK-293T cells were transfected with corresponding pGL3-Basic constructs, renilla and miR-23b-3p mimic (or scramble control) using Lipofectamin 3000 in 24-well plate. The cells were harvested after transfection for 36h and the luciferase activity was measured using TransDetect Double-Luciferase Reporter Assay Kit (TransGen Biotech Ltd., Beijing, China) according to the manufacturer's instruction. Renilla activities were measured as internal control. Data were obtained by normalization of renilla activity to luciferase activity.

2.12. Statistical analysis

SPSS 19.0 statistical software and Graphpad graphing software were used for statistical analysis and graphing of quantitative PCR results. Data were expressed as mean ± standard deviation, and paired *t*-test was used to compare the differences between cancer and paracancer. The relationship of Lnc-PLA2G4A-4 with clinicopathological characteristics was analyzed using the chi-square test or Fisher's exact probability method. The differences of overall patient survival and relapse-free survival with high or low expression level of Lnc-PLA2G4A-4 were estimated using the Kaplan-Meyer method, and the log-rank test was performed to examine the significance. Comparisons between the two samples were made using paired or unpaired t-tests for measurement data, and one-way ANOVA was used for comparisons between categorical and count data. Lung metastases in mice were counted by counting the number of lung nodules using the nonparametric *U* test. $p < 0.05$ was considered a statistically significant difference in the analysis.

3. Results

3.1. Lnc-PLA2G4A-4 was up-regulated in HCC tissues and relates to worse prognosis

Various lncRNAs are reported to be involved in cancer development. However, the specific lncRNAs to engage in HCC progression is yet to be explored. In our previous study, we performed RNA transcriptome sequencing analysis in 61 paired HCC tissues and corresponding para-tumor tissues and found that Lnc-PLA2G4A-4 (AL596211.1) was one of up-regulated lncRNAs in HCC tissues [23]. So far, the study of lnc-PLA2G4A-4 in HCC has not been reported, therefore we were particularly focused on this uncharacterized lncRNA. In this study, we are intended to provide novel insights into the mechanism of HCC and potentially explore important

therapeutic implications for HCC treatment. We wanted to explore the clinical significance and molecular mechanism of Lnc-PLA2G4A-4 in HCC. To further verify the RNA transcriptome sequencing analysis result, we expanded the sample size to measure the expression of Lnc-PLA2G4A-4. Total RNAs from 105 pairs of HCC tissues and adjacent normal tissues were extracted and confirmed that Lnc-PLA2G4A-4 expression was significantly up-regulated in HCC tissues by RT-qPCR with unpaired (Fig. 1A) and paired t-tests (Fig. 1B). The up-regulation of Lnc-PLA2G4A-4 was also observed in the TCGA dataset with unpaired (Fig. 1C) and paired t-tests (Fig. 1D). Thereafter, the up-regulation of Lnc-PLA2G4A-4 in HCC tissue was also confirmed by Fluorescence in Situ Hybridization (FISH) assay (Fig. 1E). More importantly, Kaplan-Meier analysis indicated that high expression of Lnc-PLA2G4A-4 is associated with shorter overall survival ($p = 0.0363$, Fig. 1F) and recurrence free survival ($p = 0.0424$, Fig. 1F). Further clinical pathology data analysis shows that the increased expression of Lnc-PLA2G4A-4 significantly correlated with the tumor size and microvascular invasion of patients (Table 1). Collectively, these data suggest that increased Lnc-PLA2G4A-4 level in tumor associates with poor clinical outcomes of HCC patients.

3.2. *Lnc-PLA2G4A-4 promotes HCC cell proliferation*

Consider that Lnc-PLA2G4A-4 was up-regulated in HCC tissue; we next investigated the effects of Lnc-PLA2G4A-4 on HCC cell phenotypes. First of all, the expression of Lnc-PLA2G4A-4 was evaluated in seven wild-type HCC cell lines (SNU398, SNU449, SK-Hep-1, Hep3B, Huh7, SMMC-7721, HepG2) and found that SMMC-7721 cells showed higher background levels of Lnc-PLA2G4A-4 than other 6 other cell lines (Fig. 2A). Thus Lnc-PLA2G4A-4 was stably over-expression in SNU398, C3A and SK-Hep-1 cells and knocked down in SMMC-7721 cells respectively. The over-expression and knockdown of Lnc-PLA2G4A-4 were confirmed by RT-qPCR (Fig. 2B). Notably, compared with those in corresponding control cells, proliferation and colony formation were both increased in the Lnc-PLA2G4A-4 over-expressed SNU398 or SK-Hep-1 cells and reduced in Lnc-PLA2G4A-4 knockdown SMMC-7721 cells (Fig. 2C and D and Supplementary Figs. S1 and S2). Previous studies show that AKT signaling is a critical signal transduction pathway that regulates cell proliferation [24]. Among them, AKT/p21 signaling cascade promotes cancer cells proliferation was reported by many researches [25,26]. We next examined the expression of the significant markers related to the AKT signaling pathways in HCC cells with

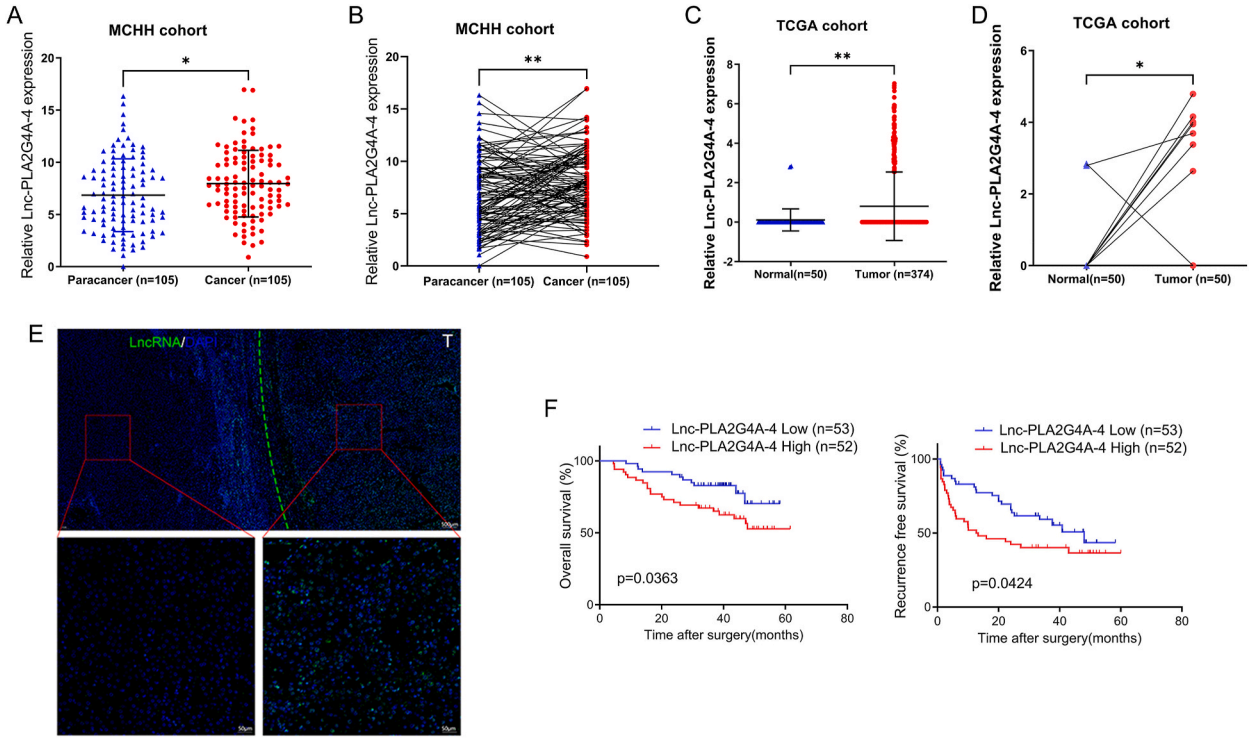

Fig. 1. Lnc-PLA2G4A-4 was up-regulated in HCC tissues. A. RT-qPCR validation of Lnc-PLA2G4A-4 expression in 105 HCC patients with paired tumor and para-tumor tissues. 18S rRNA was used as an internal control. Student's unpaired *t*-test was used to compare the difference between para-tumor and tumor tissues. **B.** Relative expression level of Lnc-PLA2G4A-4 in adjacent para-tumor tissues (n = 105) and HCC tumor tissues (n = 105) from MCHH in Student's paired *t*-test. **C.** Relative expression level of Lnc-PLA2G4A-4 in normal liver tissues (n = 50) and HCC tumor tissues (n = 374) from TCGA cohort in Student's unpaired *t*-test. **D.** Relative expression level of Lnc-PLA2G4A-4 in normal liver tissues (n = 50) and HCC tumor tissues (n = 50) from TCGA cohort in Student's paired *t*-test. **E.** Fluorescence in Situ Hybridization (FISH) assay (green) used to examine the expression of Lnc-PLA2G4A-4 in HCC tissue. **F.** Kaplan–Meier analysis revealed that high expression of Lnc-PLA2G4A-4 significantly associated with shorter OS (overall survival) and RFS (recurrence free survival). (For interpretation of the references to colour in this figure legend, the reader is referred to the Web version of this article.)

Table 1
Correlation between the clinicopathological characteristics and Lnc-PLA2G4A-4 expression in HCC.

Parameter	No.of patients	Lnc-PLA2G4A-4		c^2-value	*P* value
		Low (n = 53)	High (n = 52)		
Sex					
male	85	41	44	0.896	0.344
female	20	12	8		
Age (year)					
< 55	56	32	24	2.134	0.144
≥55	49	21	28		
Tumor size (cm)					
< 5	58	35	23	5.048	**0.025***
≥5	47	18	29		
Microvascular invasion					
Yes	46	18	28	4.216	**0.040***
No	59	35	24		
Tumor capsule					
Yes	91	45	46	0.287	0.592
No	14	8	6		
Tumor number					
Single	102	51	51	0.324	0.569
Multiple	3	2	1		
AFP (ng/ml)					
≤400	73	40	33	1.787	0.181
>400	32	13	19		
Differentiation grade					
I-II	34	19	15	0.489	0.484
III-IV	70	34	36		
TNM stage					
I-II	84	46	38	3.086	0.079
III-IV	21	7	14		
Liver cirrhosis					
yes	84	46	38	3.086	0.079
no	21	7	14		
Hepatitis B					
Yes	96	48	48	0.102	0.750
No	9	5	4		

Lnc-PLA2G4A-4 over-expression or knockdown by Western blot. As shown in Fig. 2E, Lnc-PLA2G4A-4 over-expression in SK-Hep-1 cells enhanced the expression of p-AKT and cyclin D1 at the protein level, whereas Lnc-PLA2G4A-4 knockdown in SMMC-7721 cells reduced the protein level of p-AKT and cyclin D1. Lnc-PLA2G4A-4 expression had the adverse effects on the expression of p21, which is a cyclin-dependent kinase inhibitor [27]. Hence, Lnc-PLA2G4A-4 regulates cell proliferation through AKT/p21 signaling pathway.

3.3. Lnc-PLA2G4A-4 regulates HCC cell migration and invasion in vitro and in vivo

Moreover, cell migration and invasion abilities in HCC cell lines were also significantly increased by Lnc-PLA2G4A-4 over-expression and suppressed by Lnc-PLA2G4A-4 knockdown (Fig. 3A). The wound healing assays validate that Lnc-PLA2G4A-4 positively regulates cell migratory capacity both in HepG2/C3A and SMMC-7721 cells (Fig. 3B). In addition, when cells were pretreated with cell cycle inhibitor mitomycin C to block proliferation, Lnc-PLA2G4A-4 over-expression can still promotes migration and invasion of HCC cell (Supplementary Fig. S3). EMT is well known to be involved in the invasion and metastasis of cancer cells [28]. In addition, we examined the expression of the significant markers related to EMT in HCC cells with Lnc-PLA2G4A-4 over-expression or knockdown by Western blot. The result showed that Lnc-PLA2G4A-4 decreased the expression of epithelial marker E-cadherin, but increased mesenchymal markers N-cadherin and Vimentin as well as EMT-inducing transcription factor snail, slug and ZEB2. Conversely, Lnc-PLA2G4A-4 knockdown in SMMC-7721 cells induced a reverse trend (Fig. 3C). To further validate the function of Lnc-PLA2G4A-4 in metastasis of HCC in vivo, a lung metastasis mouse model was constructed and the results showed that Lnc-PLA2G4A-4 knockdown dramatically inhibited HCC lung metastasis of SMMC-7721 cells (Fig. 3D and E).

3.4. Lnc-PLA2G4A-4 acts as a molecular sponge for miR-23b-3p in HCC cells

To further determine the subcellular localization of Lnc-PLA2G4A-4, fluorescence in situ hybridization (FISH) assays were performed at tissue and cellular levels for the intracellular localization of Lnc-PLA2G4A-4. The cell fractionation assay was also conducted to detect the distribution of lnc-PLA2G4A-4. The results demonstrated that Lnc-PLA2G4A-4 is localized in the cytoplasm (Fig. 4A and B) which meant Lnc-PLA2G4A-4 may act as sponge to inactivate miRNAs and thus regulate the post-transcriptional translation of target genes. To investigate the mechanisms underlying the role of Lnc-PLA2G4A-4 in HCC, we predicted the possible binding microRNAs of Lnc-PLA2G4A-4 by miRNA target prediction tools (LncBase, LNCediting and LncRNASNP2) and found 7 miRNAs that

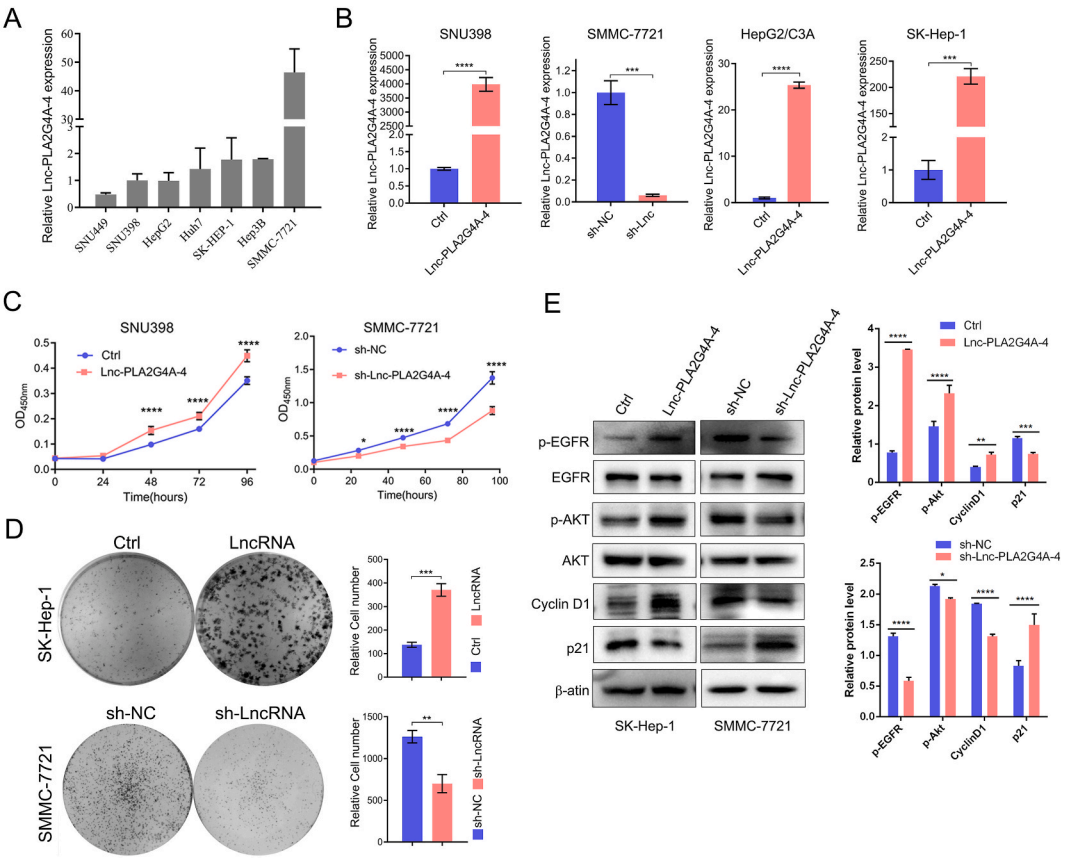

Fig. 2. Lnc-PLA2G4A-4 regulates HCC cell proliferation. A. Relative expression of Lnc-PLA2G4A-4 in different HCC cell lines. **B.** Validation of Lnc-PLA2G4A-4 over-expression and knockdown effect in different HCC cell lines. **C, D.** The CCK8 assays and colony formation assays detection of cellular growth in SNU398 cells with Lnc-PLA2G4A-4 over-expression or SMMC-7721 cells with Lnc-PLA2G4A-4 knockdown, respectively. **E.** Western blotting detection of protein expression of p-EGFR, EGFR, p-AKT, AKT, cyclin D1 and p21 in stable up-regulation or down-regulation of Lnc-PLA2G4A-4.

may bind to Lnc-PLA2G4A-4 (Fig. 4C). Therefore, miR-567, miR-888 and miR-23b-3p were selected for validation using luciferase reporter assays. As shown in Fig. 4D, miR-23b-3p was a potential target of Lnc-PLA2G4A-4, while miR-567 and miR-888 did not bind to Lnc-PLA2G4A-4. We constructed two types of luciferase reporter vectors containing either wild type (WT) or mutated (MUT) putative binding sites of Lnc-PLA2G4A-4 transcript to confirm miR-23b-3p is regulated by Lnc-PLA2G4A-4. In luciferase reporter assays, transfection of miR-23b-3p significantly inhibited the luciferase activity in HEK-293T cells but failed to regulate the luciferase activity when the binding site was mutated (Fig. 4E), which indicated that miR-23b-3p directly bind to Lnc-PLA2G4A-4. Next, the expression levels of miR-23b-3p were evaluated in five HCC cell lines (Huh7, SNU398, SMMC-7721, SK-Hep-1, HepG2) and normal human hepatocyte cell line LO2, and the data indicated that miR-23b was down-regulated in HCC cell line (Fig. 4F). In addition, the down-regulation of miR-23b-3p was also observed in the TCGA dataset (Fig. 4G and H). Moreover, Lnc-PLA2G4A-4 over-expression significantly decreased the expression of miR-23b-3p and Lnc-PLA2G4A-4 knock-down improved the expression of miR-23b-3p (Fig. 4I). Finally, we examined the correlation between miR-23b-3p and Lnc-PLA2G4A-4 expression in HCC samples from 32 patients at MCHH (Fig. 4J) and form TCGA cohort (Fig. 4K). Therefore, the expression of the miR-23b-3p was significantly negatively correlated with Lnc-PLA2G4A-4 in HCC cells and tissues. Hence, the above data indicated that Lnc-PLA2G4A-4 directly bind to miR-23b-3p.

3.5. Lnc-PLA2G4A-4 promotes HCC cell proliferation, migration and invasion by sponging miR-23b-3p

To determine whether Lnc-PLA2G4A-4 regulates HCC cells phenotypic changes by sequestering miR-23b-3p, we performed transwell assays and the results revealed that the effect of Lnc-PLA2G4A-4 on SNU398 cells migration was rescued by co-transfection of miR-23b (Fig. 5A). Conversely, Lnc-PLA2G4A-4 knock-down on SMMC-7721 cells migration was rescued by co-transfection of miR-23b inhibitor (Fig. 5B). The results of wound healing assays indicated that Lnc-PLA2G4A-4 abolished the inhibiting effect of migration and invasion by "sponge" adsorption of miR-23b (Fig. 5C and D). In addition, CCK-8 cell proliferation assays showed the effect of Lnc-PLA2G4A-4 over-expression on HCC cells proliferation was rescued by co-transfection of miR-23b (Fig. 5E). Hence, Lnc-PLA2G4A-

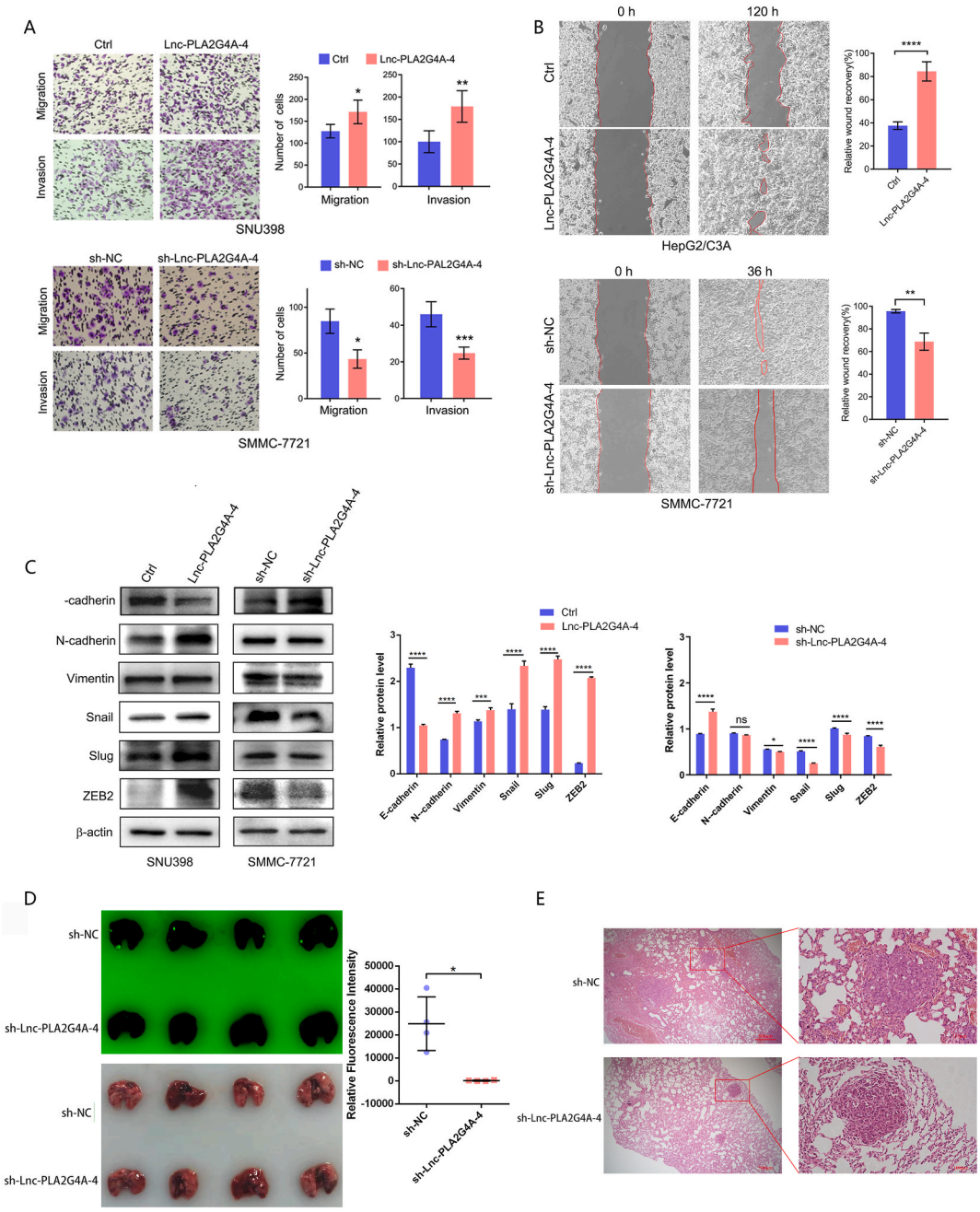

Fig. 3. Lnc-PLA2G4A-4 promotes HCC cell migration and invasion in vitro and in vivo. A. Representative and quantification results of transwell cell migration and invasion assays in Lnc-PLA2G4A-4 over-expression cells or Lnc-PLA2G4A-4 knockdown cells. **B.** The wound healing assays detection of cellular growth in SNU398 cells with Lnc-PLA2G4A-4 over-expression or SMMC-7721 cells with Lnc-PLA2G4A-4 knockdown, respectively. **C.** Western blotting detection of epithelial, mesenchymal and transcription factors in Lnc-PLA2G4A-4 over-expression cells or Lnc-PLA2G4A-4 knockdown cells, respectively. **D.** Representative images and quantification data of metastatic nodules in the lung tissues of mice. Stable cell lines of sh-Lnc-PLA2G4A-4 or sh-NC were injected by tail vein in B-NSG mice. Left: macroscopic and fluorescent images. Right: quantification data of lung metastatic nodules. **E.** Representative images of lung metastatic nodules stained with H&E (magnification,×50 and × 200; scale bar, 500 and 100 μm).

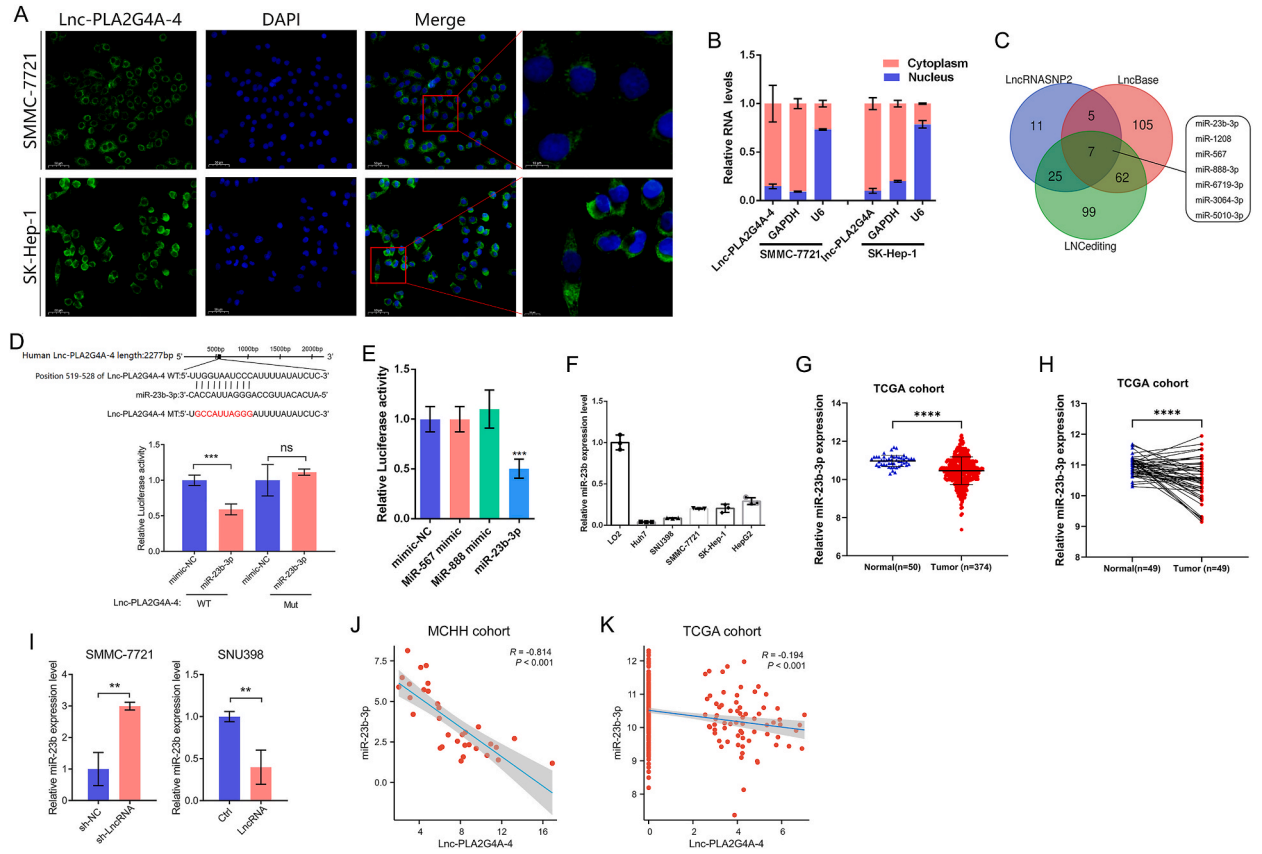

Fig. 4. Lnc-PLA2G4A-4 directly binds to miR-23b-3p. A. Fluorescence in Situ Hybridization assay used to examine the expression and location of Lnc-PLA2G4A-4 in SMMC-7721 and SK-Hep-1 cells. **B.** Cell fractionation assay used to examine the location of Lnc-PLA2G4A-4 in SMMC-7721 and SK-Hep-1 cells. **C.** The predicted results of Lnc-PLA2G4A-4 downstream target genes from three databases. **D.** Relative luciferase activities in 293T cells co-transfected with the mimic-NC/miR-567 mimic/miR-888 mimic/miR-23b-3p mimic and Lnc-PLA2G4A-4-WT reporter vector. **E.** Up: prediction of miR-23b-3p binding sites in Lnc-PLA2G4A-4 (Lnc-PLA2G4A-4-WT) and the design of Lnc-PLA2G4A-4 mutation sequence (Lnc-PLA2G4A-4-Mut). Down: luciferase reporter assays were performed in 293T cells co-transfected with the miR-23b-3p mimic and Lnc-PLA2G4A-4-WT or Lnc-PLA2G4A-4-Mut reporter vector. **F.** Relative expression of miR-23b in different HCC cell lines. **G.** Expression of miR-23b-3p in 50 normal tissue and 374 HCC tumor tissue from TCGA cohort in Student's unpaired *t*-test. **H.** Expression of miR-23b in 49 normal tissue and 49 HCC tumor tissue from TCGA cohort in Student's paired *t*-test. **I.** Relative expression of miR-23b in Lnc-PLA2G4A-4 over-expression cells or Lnc-PLA2G4A-4 knockdown cells, respectively. **J.** Correlation between miR-23b-3p and Lnc-PLA2G4A-4 expression in HCC tissues of MCHH. **K.** Correlation between miR-23b-3p and Lnc-PLA2G4A-4 expression in HCC tissues of TCGA.

4 regulates HCC cell proliferation and metastasis via sponging miR-23b-3p.

3.6. MiR-23b-3p/versican axis mediates the pro-oncogenic action of Lnc-PLA2G4A-4 in HCC

The above data have confirmed that Lnc-PLA2G4A-4 promotes HCC cell proliferation, migration and invasion by sponging miR-23b-3p. However, how Lnc-PLA2G4A-4/miR-23b axis regulates HCC progression still need to further explore. To identify the underlying molecular mechanism, RNA transcriptome sequencing was performed in Lnc-PLA2G4A-4 over-expression cells and control cells were. As shown in Fig. 6A, Supplementary Table S3 and Supplementary data S4, there are 64 genes up-regulated and 48 genes down-regulated in Lnc-PLA2G4A-4 over-expression cells. Among the higher-ranking upregulated genes, we noticed that versican (VCAN) was significantly up-regulated. It has been reported that versican was a downstream target of miR-23b-3p [29], and participating in the regulation of proliferation and metastasis of cancers. Therefore, we guess Lnc-PLA2G4A-4 may play its pro-oncogenic role via miR-23b-3p/Versican axis. In addition, TCGA dataset supported the upregulation of versican in HCC tissues (Fig. 6B and C) and high expression of versican was related to worse prognosis (Fig. 6D). Correspondingly, Pearson's correlation analysis indicated that there is a negatively correlation between expression of versican with miR-23b-3p (Fig. 6E and F) and a positive correlation between expression of versican and Lnc-PLA2G4A-4 (Fig. 6G and H), which was analyzed using the MCHH tissues and the TCGA dataset. To further confirm the positive correlation between versican and Lnc-PLA2G4A-4, we investigate the effects of Lnc-PLA2G4A-4 on the expression of versican mRNA and protein by RT-qPCR and Western blot. The result showed that Lnc-PLA2G4A-4 can positively regulate versican expression at the mRNA and protein levels (Fig. 6I and J), while miR-23b negatively

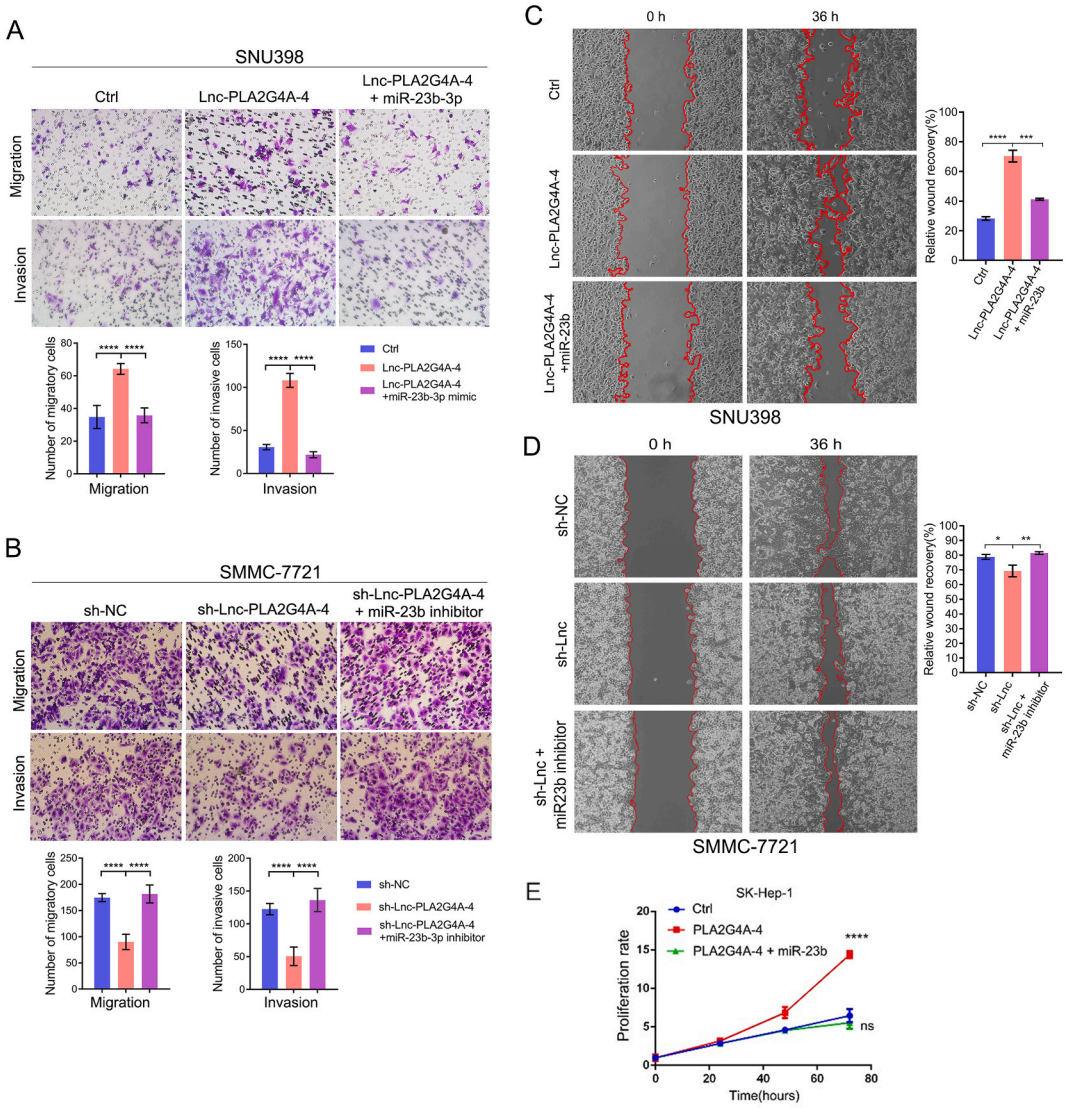

Fig. 5. Lnc-PLA2G4A-4 promotes HCC cell proliferation, migration and invasion by sponging miR-23b. A, B. Transwell assays detected Lnc-PLA2G4A-4 can reverse the effect of miR-23b-3p on the migration and invasion ability of HCC cells. **C, D.** wound-healing assays detected Lnc-PLA2G4A-4 can reverse the effect of miR-23b-3p on the migration and invasion ability of SNU-398 and SMMC-7721 cells. **E.** The CCK8 assays detection of cellular growth in SK-Hep-1 cells stably transfected with Lnc-PLA2G4A-4 or co-transfected with miR-23b and Lnc-PLA2G4A-4.

regulates the expression of versican (Fig. 6K).

Simultaneously, luciferase reporter assay indicated that miR-23b binds to the 3′-untranslated region (UTR) of versican transcripts (Fig. 6L), which is consistent with the previous report [29]. Next, miR-23b-3p inhibitor was transfected in Lnc-PLA2G4A-4 knockdown SMMC-7721 cells, and Western blot assays demonstrated that miR-23b-3p inhibitor partly restore the suppressive effects of sh-Lnc-PLA2G4A-4 on EMT (Fig. 6M). Additionally, previous study has reported that versican regulates the expression level of p-EGFR and participates in regulating the proliferation of cancer cells through the p-EGFR/p-AKT signaling pathway [11]. Therefore, we examined the expression of the significant markers related to p-EGFR/p-AKT signaling pathway in HCC cells with Lnc-PLA2G4A-4 over-expression or knockdown by Western blot. The result showed that Lnc-PLA2G4A-4 over-expression in SNU398 cells enhanced the expression of p-EGFR and p-AKT at the protein level, whereas Lnc-PLA2G4A-4 knockdown in SMMC-7721 cells reduced the protein level of those proteins (Figs. 2E and 6 M). In addition, miR-23b-3p inhibitor restores the suppressive effects of sh-Lnc-PLA2G4A-4 on p-EGFR, p-AKT and versican (Fig. 6M), which indicated that Lnc-PLA2G4A-4 promoted HCC cells proliferation through the miR-23b/versican/p-EGFR/p-AKT signaling pathway. Taken together, we identified a novel lncRNA Lnc-PLA2G4A-4, which acts as an endogenous sponge of miR-23b-3p to promote HCC cell proliferation and metastasis via targeting miR-23b-3p/versican axis (Fig. 6N).

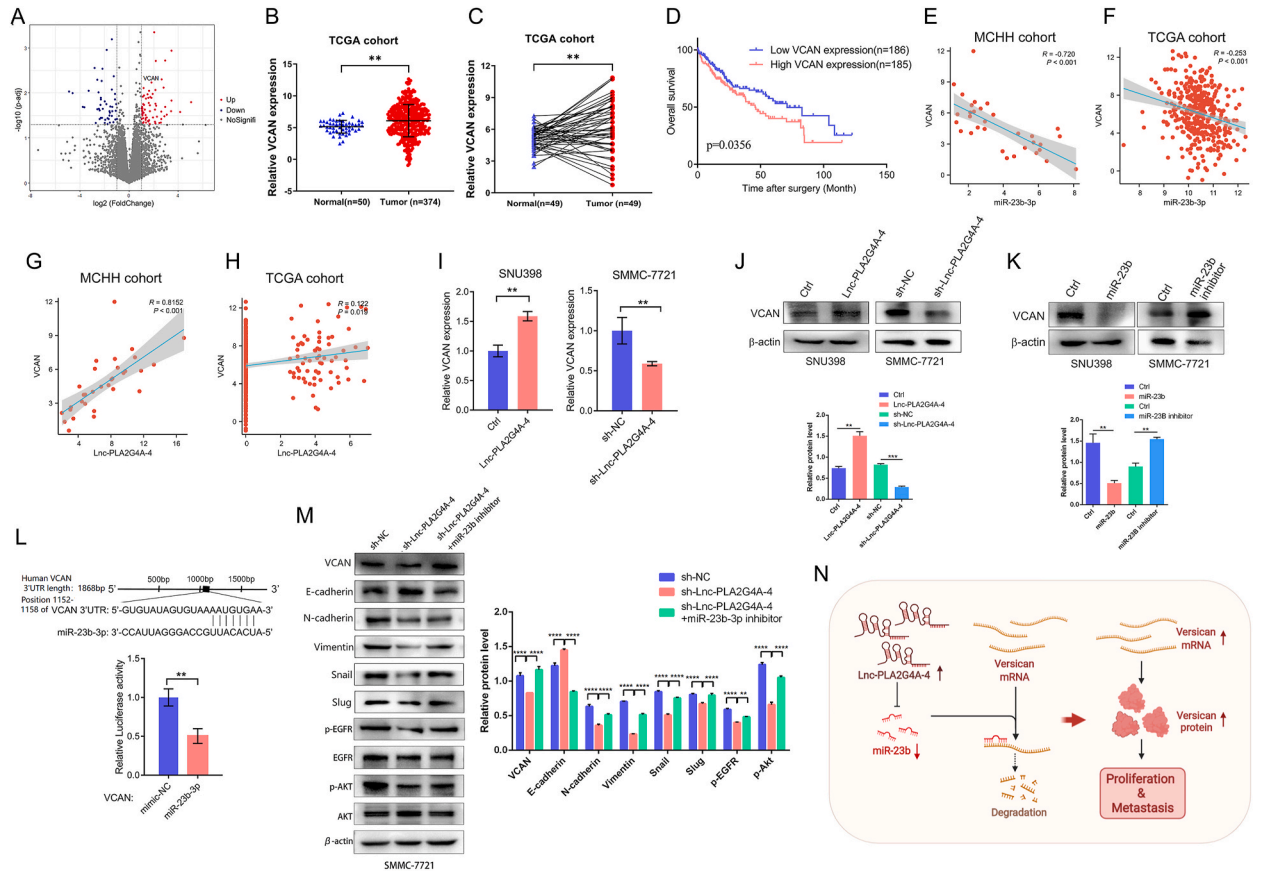

Fig. 6. The pro-oncogenic action of Lnc-PLA2G4A-4 was mediated by miR-23b-3p/versican axis. A. Volcano map of differentially expressed gene by single-cell sequence. **B, C.** Relative versican expression in paired cancer and paracancer tissues in TCGA cohort. **D.** Prognostic difference of high and low expression of versican in TCGA-LIHC cohort. **E, F.** Correlation between miR-23b-3p and versican expression in HCC tissues of MCHH and TCGA. **G, H.** Correlation between Lnc-PLA2G4A-4 and versican expression in HCC tissues of MCHH and TCGA. **I.** RT-qPCR detected Lnc-PLA2G4A-4 regulates the expression of versican. **J.** Western blot assays detected Lnc-PLA2G4A-4 regulates the expression of versican. **K.** Western blot assays detected miR-23b regulates the expression of versican. **L.** Luciferase reporter assay to verify the binding of miR-23b-3p to versican 3'UTR region. **M.** Western blotting detection of protein expression of EMT related marker, VCAN, p-EGFR, EGFR, p-AKT, AKT in SMMC-7721 cells stably transfected with sh-Lnc-PLA2G4A-4 or co-transfected with miR-23b inhibitor and sh-Lnc-PLA2G4A-4. **N.** Schematic overview of Lnc-PLA2G4A-4 contributes to hepatocellular carcinoma proliferation, migration and invasion.

4. Discussion

To date, more and more evidences have confirmed that long noncoding RNAs (lncRNAs) play important roles in the tumor progression [30], including hepatocellular carcinoma (HCC) [31]. However, there still are many functions and mechanisms of lncRNAs in the pathogenesis of HCC require further elucidation. In this study, we found a new HCC-related long non-coding RNA, Lnc-PLA2G4A-4, and elucidate its biological function and molecular mechanism in HCC development. Upregulation of Lnc-PLA2G4A-4 in HCC results in down-regulation of miR-23b, leading to enhanced versican expression and in turn accelerating tumor growth, migration and invasion.

The aberrant expression of lncRNA is involved in the regulation of HCC progression [32,33], which means lncRNAs have tremendous potential as novel biomarkers [34]. Notably, the expression level of Lnc-PLA2G4A-4 was associated with the tumor size and microvascular invasion. It's reported that microvascular invasion (MVI) has increasingly been recognized to reflect enhanced abilities of local invasion and distant metastasis of HCC [32]. Therefore, we proposed a hypothesis that Lnc-PLA2G4A-4 has potential functions of regulating tumor proliferation and metastasis in liver cancers. Next, we functionally validated this in vivo and in vitro by performing phenotypic analysis and the results are consistent with our hypothesis. Importantly, our data suggested that Lnc-PLA2G4A-4 related to worse prognosis, which highlighted Lnc-PLA2G4A-4 acted as a tumor oncogene in tumor cells abilities and its measurable values in clinical application.

The molecular mechanisms of lncRNA are closely associated with their subcellular localization. LncRNAs enriched in the nucleus typically regulate gene expression at the levels of epigenetic modification and transcription, while lncRNAs enriched in the cytoplasm typically served as the miRNA sponges to participate in post-transcriptional regulation [33]. Therefore, we explored the subcellular localization of Lnc-PLA2G4A-4 and found it was mainly localized to the cytoplasm. And many studies have demonstrated that mRNA,

lncRNA, pseudogene transcripts, circRNA can regulate the protein levels of encoded genes and the biological behavior of cells by competitively binding to miRNA [34]. Thus, we guess Lnc-PLA2G4A-4 may act as a ceRNA to promote HCC proliferation and metastasis. In our research, we identified some possible binding microRNAs of Lnc-PLA2G4A-4 by bioinformatic prediction, which were reported to regulate tumor progression, such as miR-23b, miR-567 and miR-888. Among them, miR-23b-3p attracted our attention, because it acts as both a tumor suppressor [35–37] and an oncogenic miRNA [38–40] in various types of carcinogenesis. There is accumulating evidence that miR-23b performed a variety of functions in various tumor progressions, which is involved in proliferation [41], apoptosis [42], metastasis [43], angiogenesis [44], chemoresistance [45] and glycolysis [45]. In addition, miR-23b was significantly down-regulated in LIHC dataset. Therefore, we were trying to further reveal its function and mechanism in HCC. In this study, we discovered that Lnc-PLA2G4A-4 promotes HCC proliferation and metastasis by sponging miR-23b-3p. Hence, there was a reason to believe that miR-23b-3p might play a negative role in regulating HCC proliferation and metastasis.

Versican, the downstream target genes of Lnc-PLA2G4A-4, was reported that had the functions of regulating tumor proliferation and metastasis [14,17]. According to previous research, the expression of versican is regulated by several miRNAs, such as miR-23b [29], miR-144 [46], miR-143 [47]. In combination with literature research, we wonder if Lnc-PLA2G4A-4 regulates tumor proliferation and metastasis by miR-23b-3p/versican axis. Then, our studies showed that miR-23b was able to inhibit versican expression and reverse the function of Lnc-PLA2G4A-4 in promoting HCC proliferation, invasion and migration. We also found that versican could facilitate the tumor proliferation via targeting p-EGFR/p-Akt axis and promote EMT progress, which ties well with previous studies [29]. Thus, we speculated that Lnc-PLA2G4A-4 promotes HCC progression by inducing versican expression via sponging miR-23b-3p, which expanded our understanding of the HCC progression network.

In our study, we found Lnc-PLA2G4A-4 promoted EMT via versican, which may regulate EMT via targeting E-cadherin. Nevertheless, versican may also promote EMT via other pathways. For example, the G1 domain of versican plays a role in the crosslinking of hyaluronic acid and HAPLN1, which mediated cell adhesion and proliferation [48]. As the expression of other EMT markers was also influenced by versican, the downstream signaling network of Lnc-PLA2G4A-4 in regulating EMT still needs further investigation. Recently, versican was reported to promote escaping from tumor immune surveillance through dendritic cell dysfunction [49]. Versican silencing also improves the antitumor efficacy of endostatin by alleviating its induced inflammatory and immunosuppressive changes in the tumor microenvironment [50]. Therefore, it is worth exploring whether Lnc-PLA2G4A-4 plays a key role in the tumor microenvironment through miR-23b/versican pathway.

4.1. Limitation of the study

The main drawback of the present study is the lack of in vivo data about the function of Lnc-PLA2G4A-4 in proliferation of HCC. Though we have examined that Lnc-PLA2G4A-4 regulates cell proliferation by activating the EGFR-AKT signaling, whether PLA2G4A-4 regulates cell proliferation through the versican/EGFR/AKT pathway needs to be further tested in animal models.

5. Conclusions

Our research concluded that Lnc-PLA2G4A-4 related to worse prognosis and served as a ceRNA for miR-23b-3p to facilitate the proliferation, migration and invasion of HCC through increasing versican expression. The results of our study illustrated the biological function of Lnc-PLA2G4A-4 in the progression of HCC, suggesting that Lnc-PLA2G4A-4 might be a new indicator for HCC prognosis and a potential therapeutic target of HCC.

Declarations

Ethics statement

Informed consent was obtained from all patients for the publication of all their data and/or images included within the paper and this study was approved by the ethics committee of Mengchao Hepatobiliary Hospital of Fujian Medical University (2020-027-01). All animal experiments were approved by the ethics committee of the Laboratory Animal Center of Fujian Medical University (FJMU 1ACUC 2021-0321).

Author contributions

Jiahui Xiong; Jizhe Liu: Performed the experiments; Analyzed and interpreted the data; Wrote the paper.
Yongping Lai; Niangmei Cheng; Fei Wang; Xiaoyuan Zheng; Yantin Lin: Performed the experiments.
Yingchao Wang, Qiuyu Zhuang, Yixuan Yang: Analyzed and interpreted the data.
Jingfeng Liu: Analyzed and interpreted the data; Contributed reagents, materials, analysis tools or data.
Bixing Zhao: Conceived and designed the experiments; analyzed and interpreted the data; Wrote the paper.
Xiaoyu Yang: Conceived and designed the experiments; analyzed and interpreted the data.

Funding statement

This work was supported by the National Natural Science Foundation of China (81972714), the Natural Science Foundation of

Fujian Province (2020J011159, 2019J01140, 2022L3030, 2021Y9032, 2023J011467), the Scientific Foundation of Fuzhou City (2021-S-098, 2021-S-100), the Scientific Foundation of Fuzhou Municipal Health Commission (2021-S-wt2, 2021-S-wp1), the Scientific Foundation of Fujian Provincial Health Commission (2021QNA063, 2020QNA072).

Data availability statement

The data used for supporting the findings of this study are available from the corresponding authors upon request.

Declaration of competing interest

The authors declare that they have no known competing financial interests or personal relationships that could have appeared to influence the work reported in this paper.

Appendix A. Supplementary data

Supplementary data to this article can be found online at https://doi.org/10.1016/j.heliyon.2023.e18698.

References

[1] C. de Martel, J. Ferlay, S. Franceschi, et al., Global burden of cancers attributable to infections in 2008: a review and synthetic analysis, the Lancet, Oncology 13 (2012) 607–615.
[2] Z. Tang, S. Ye, Y. Liu, et al., A decade's studies on metastasis of hepatocellular carcinoma, J. Cancer Res. Clin. Oncol. 130 (2004) 187–196.
[3] E. Anastasiadou, L. Jacob, F. Slack, Non-coding RNA networks in cancer, Nat. Rev. Cancer 18 (2018) 5–18.
[4] Z. Chen, L. Huang, Y. Wu, et al., LncSox4 promotes the self-renewal of liver tumour-initiating cells through Stat3-mediated Sox4 expression, Nat. Commun. 7 (2016), 12598.
[5] P. Monnier, C. Martinet, J. Pontis, et al., H19 lncRNA controls gene expression of the Imprinted Gene Network by recruiting MBD1, Proc. Natl. Acad. Sci. U. S. A 110 (2013) 20693–20698.
[6] C. Chu, Q. Zhang, S. da Rocha, et al., Systematic discovery of Xist RNA binding proteins, Cell 161 (2015) 404–416.
[7] M. Huarte, The emerging role of lncRNAs in cancer, Nat. Med. 21 (2015) 1253–1261.
[8] J. Pu, H. Wei, C. Tan, et al., Long noncoding RNA SNHG14 facilitates hepatocellular carcinoma progression through regulating miR-4673/SOCS1, Am. J. Tourism Res. 11 (2019) 5897–5904.
[9] S. Li, Y. Zhu, R. Li, et al., αLncRNA lnc-APUE is repressed by HNF4 and promotes G1/S phase transition and tumor growth by regulating MiR-20b/E2F1 Axis, Adv. Sci. 8 (2021), 2003094.
[10] W. Du, W. Yang, A. Yee, Roles of versican in cancer biology–tumorigenesis, progression and metastasis, Histol. Histopathol. 28 (2013) 701–713.
[11] G. Zhangyuan, F. Wang, H. Zhang, et al., VersicanV1 promotes proliferation and metastasis of hepatocellular carcinoma through the activation of EGFR-PI3K-AKT pathway, Oncogene 39 (2020) 1213–1230.
[12] D. Brunn, K. Turkowski, S. Günther, et al., Interferon regulatory factor 9 promotes lung cancer progression via regulation of versican, Cancers 13 (2021).
[13] A. Yee, M. Akens, B. Yang, et al., The effect of versican G3 domain on local breast cancer invasiveness and bony metastasis, Breast Cancer Res. 9 (2007) R47.
[14] L. Zhai, W. Chen, B. Cui, et al., Overexpressed versican promoted cell multiplication, migration and invasion in gastric cancer, Tissue Cell 73 (2021), 101611.
[15] J. Guo, Y. Liu, INHBA promotes the proliferation, migration and invasion of colon cancer cells through the upregulation of VCAN, J. Int. Med. Res. 49 (2021), 3000605211014998.
[16] W. Liu, W. Wang, N. Zhang, et al., The role of CCL20-CCR6 Axis in ovarian cancer metastasis, OncoTargets Ther. 13 (2020) 12739–12750.
[17] Q. Zhang, J. Wu, X. Chen, et al., Upregulation of versican associated with tumor progression, metastasis, and poor prognosis in bladder carcinoma, BioMed Res. Int. 2021 (2021), 6949864.
[18] C. Ricciardelli, A. Sakko, M. Ween, et al., The biological role and regulation of versican levels in cancer, Cancer Metastasis Rev. 28 (2009) 233–245.
[19] R. Li, S. Hou, M. Zou, et al., miR-543 impairs cell proliferation, migration, and invasion in breast cancer by suppressing VCAN, Biochem. Biophys. Res. Commun. 570 (2021) 191–198.
[20] X. Zhao, Z. Sun, H. Li, et al., MiR-135a-5p modulates biological functions of thyroid carcinoma cells via targeting VCAN 3'-UTR, Cancer biomarkers : section, Dis. Markers 20 (2017) 207–216.
[21] X. Wang, G. Hu, J. Zhou, Repression of versican expression by microRNA-143, J. Biol. Chem. 285 (2010) 23241–23250.
[22] Y. Wang, J. Tan, C. Xu, et al., Identification and construction of lncRNA-associated ceRNA network in diabetic kidney disease, Medicine 100 (2021), e26062.
[23] B. Zhao, K. Ke, Y. Wang, et al., HIF-1α and HDAC1 mediated regulation of FAM99A-miR92a signaling contributes to hypoxia induced HCC metastasis, Signal Transduct. Targeted Ther. 5 (2020) 118.
[24] G. Hoxhaj, B. Manning, The PI3K-AKT network at the interface of oncogenic signalling and cancer metabolism, Nat. Rev. Cancer 20 (2020) 74–88.
[25] R. Krishnan, M. Murugiah, N. Lakshmi, et al., Guanine nucleotide binding protein like-1 (GNL1) promotes cancer cell proliferation and survival through AKT/p21 signaling cascade, Mol. Biol. Cell 31 (2020) 2904–2919.
[26] T. Chen, H. Huang, Y. Zhou, et al., HJURP promotes hepatocellular carcinoma proliferation by destabilizing p21 via the MAPK/ERK1/2 and AKT/GSK3β signaling pathways, J. Exp. Clin. Cancer Res. : CR 37 (2018) 193.
[27] T. Abbas, A. Dutta, p21 in cancer: intricate networks and multiple activities, Nat. Rev. Cancer 9 (2009) 400–414.
[28] A. Dongre, R. Weinberg, New insights into the mechanisms of epithelial-mesenchymal transition and implications for cancer, Nat. Rev. Mol. Cell Biol. 20 (2019) 69–84.
[29] T. Wei, X. Cong, X. Wang, et al., Interleukin-17A promotes tongue squamous cell carcinoma metastasis through activating miR-23b/versican pathway, Oncotarget 8 (2017) 6663–6680.
[30] A. Sayad, M. Taheri, S. Arsang-Jang, et al., Hepatocellular carcinoma up-regulated long non-coding RNA: a putative marker in multiple sclerosis, Metab. Brain Dis. 34 (2019) 1201–1205.
[31] P. Zhu, Y. Wang, J. Wu, et al., LncBRM initiates YAP1 signalling activation to drive self-renewal of liver cancer stem cells, Nat. Commun. 7 (2016), 13608.
[32] X. Zhang, J. Li, F. Shen, et al., Significance of presence of microvascular invasion in specimens obtained after surgical treatment of hepatocellular carcinoma, J. Gastroenterol. Hepatol. 33 (2018) 347–354.
[33] J. Li, C. Huang, Y. Zou, et al., CircTLK1 promotes the proliferation and metastasis of renal cell carcinoma by sponging miR-136-5p, Mol. Cancer 19 (2020) 103.
[34] C. Ponting, P. Oliver, W. Reik, Evolution and functions of long noncoding RNAs, Cell 136 (2009) 629–641.

[35] J. Hu, Z. Sun, K. Hu, et al., [Over-expression of Hsa-miR-23b-3p suppresses proliferation, migration, invasion and epithelial-mesenchymal transition of human cervical cancer CasKi cells], Xi bao yu fen zi mian yi xue za zhi, Chin. J. Cell. Mol. Immun. 36 (2020) 983–989.
[36] G. Lei, Z. Li, Y. Li, et al., Long noncoding RNA FAM66C promotes tumor progression and glycolysis in intrahepatic cholangiocarcinoma by regulating hsa-miR-23b-3p/KCND2 axis, Environ. Toxicol. 36 (2021) 2322–2332.
[37] X. Yang, G. Wu, F. Yang, et al., Elevated LINC00909 promotes tumor progression of ovarian cancer via regulating the miR-23b-3p/MRC2 Axis, Oxid. Med. Cell. Longev. 2021 (2021), 5574130.
[38] L. Fan, X. Cao, Y. Lei, MicroRNA miR-23b-3p promotes osteosarcoma by targeting ventricular zone expressed PH domain-containing 1 (VEPH1)/phosphatidylinositol 3-kinase/protein kinase B (PI3K/AKT) pathway, Bioengineered 12 (2021) 12568–12582.
[39] L. Hao, Y. Yun, R. Liang, et al., Long non-coding RNA TUSC7 suppressed colorectal cancer progression via regulation of miR-23b/PDE7A Axis, Clinical and investigative medicine, Méd. Clin. Exp. 43 (2020) E35–E43.
[40] L. Wang, Z. Hu, Q. Guo, et al., MiR-23b functions as an oncogenic miRNA by downregulating Mcl-1S in lung cancer cell line A549, J. Biochem. Mol. Toxicol. 34 (2020), e22494.
[41] G. Li, Z. Zhang, Z. Chen, et al., LncRNA DLEU2 is activated by STAT1 and induces gastric cancer development via targeting miR-23b-3p/NOTCH2 axis and Notch signaling pathway, Life Sci. 277 (2021), 119419.
[42] G. Huang, Y. Yang, M. Lv, et al., miR-23b-3p inhibits the oncogenicity of colon adenocarcinoma by directly targeting NFE2L3, J. Oncol. 2021 (2021), 8493225.
[43] X. Yan, M. Zhang, B. Li, et al., RAI14 regulated by circNFATC3/miR-23b-3p axis facilitates cell growth and invasion in gastric cancer, Cell Transplant. 30 (2021), 9636897211007055.
[44] R. Lv, J. Yu, Q. Sun, viaAnti-angiogenic role of microRNA-23b in melanoma by disturbing NF-κB signaling pathway targeted inhibition of, Future Oncol. 16 (2020), 541-458.
[45] Z. Zeng, Y. Zhao, Q. Chen, et al., Hypoxic exosomal HIF-1α-stabilizing circZNF91 promotes chemoresistance of normoxic pancreatic cancer cells via enhancing glycolysis, Oncogene 40 (2021) 5505–5517.
[46] N. Gupta, R. Kumar, A. Sharma, Inhibition of miR-144/199 promote myeloma pathogenesis via upregulation of versican and FAK/STAT3 signaling, Mol. Cell. Biochem. 476 (2021) 2551–2559.
[47] F. Li, S. Li, T. Cheng, TGF-β1 promotes osteosarcoma cell migration and invasion through the miR-143-versican pathway, Cellular physiology and biochemistry, Int. J. Exp. Cell. Phys. Biochem. Pharm. 34 (2014) 2169–2179.
[48] L. Ang, Y. Zhang, L. Cao, et al., Versican enhances locomotion of astrocytoma cells and reduces cell adhesion through its G1 domain, J. Neuropathol. Exp. Neurol. 58 (1999) 597–605.
[49] A. Papadas, F. Asimakopoulos, Versican in the tumor microenvironment, Adv. Exp. Med. Biol. 1272 (2020) 55–72.
[50] Z. Wang, Z. Li, Y. Wang, et al., Versican silencing improves the antitumor efficacy of endostatin by alleviating its induced inflammatory and immunosuppressive changes in the tumor microenvironment, Oncol. Rep. 33 (2015) 2981–2991.